PHYSICAL REVIEW A VOLUME 45, NUMBER 4 15 FEBRUARY 1992

Transport coefficients of hard-sphere mixtures. II. Diameter ratio 0.4 and mass ratio 0.03 at low density

Jerome J. Erpenbeck
Los Alamos National Laboratory, Los Alamos, New Mexico 87545

(Received 23 September 1991)

The transport coefficients of shear viscosity, thermal conductivity, thermal diffusion, and mutual diffusion are estimated for a binary, equimolar mixture of hard spheres having a diameter ratio of 0.4 and a mass ratio of 0.03 at volumes of $5V_0$, $10V_0$, and $20V_0$ (where $V_0=\frac{1}{2}\sqrt{2}N\sum_a x_a\sigma_a^3$, x_a are mole fractions, σ_a are diameters, and N is the number of particles) through Monte Carlo, molecular-dynamics calculations using the Green-Kubo formulas. Calculations are reported for as few as 108 and as many as 4000 particles, but not for each value of the volume. Both finite-system and long-time-tail corrections are applied to obtain estimates of the transport coefficients in the thermodynamic limit; corrections of both types are found to be small. The results are compared with the predictions of the revised Enskog theory and the linear density corrections to that theory are reported. The mean free time is also computed as a function of density and the linear and quadratic corrections to the Boltzmann theory are estimated. The mean free time is also compared with the expression from the Mansoori-Carnahan-Starling-Leland equation of state.

PACS number(s): 51.10.+y, 05.60.+w, 66.10.−x, 66.20.+d

I. INTRODUCTION

The Enskog theory remains the only molecular-level theory of transport properties in liquids and gases. Although the theory was formulated for hard spheres, it has been extended to soft potentials in a number of distinct ways, with some measure of success. Thus the theory potentially provides a unifying description of transport in a wide range of fluids.

In view of this role, it is clearly important that the accuracy of the theory in describing the hard-sphere fluid itself be well understood. Thus, from the very earliest days of computer simulation of fluid transport properties, the question of the adequacy of the Enskog theory has been addressed. Alder, Gass, and Wainwright (AGW) used molecular-dynamics (MD) calculations based on the Green-Kubo formulas to compute the self-diffusion coefficient, the bulk and shear viscosity, and the thermal conductivity of hard spheres over much of the fluid regime [1]. In the case of self-diffusion, they discovered a large positive deviation in the dense-fluid regime, having its origin in the slow, algebraic decay of the Green-Kubo time-correlation function for self-diffusion, the velocity autocorrelation function (VACF), which was later studied extensively by means of molecular dynamics calculations by Erpenbeck and Wood both for hard disks [2] and hard spheres [3]. While the self-diffusion coefficient appears to be infinite for hard disks, for hard spheres it shows strong deviations from the Enskog theory, both positive and negative depending on density [4].

In the case of shear viscosity, AGW reported excellent agreement with the Enskog theory for hard spheres at densities appreciably below the fluid-solid phase transition and strong positive deviations near that transition which have been investigated in greater detail by Erpenbeck and Wood [5], who found these deviations to arise from the so-called cross and potential parts of the Green-Kubo time-correlation function, rather than the kinetic term which appears, both from theory [6–9] and computer simulation [5] to have an algebraic time decay, similar in form to that of the VACF but of inconsequential magnitude. Some progress in understanding the dominant deviations from the Enskog theory has been made by Kirkpatrick [10] and van Beijeren [11,12]. For thermal conductivity and bulk viscosity, the AGW calculations showed good agreement with the Enskog theory over the entire fluid regime.

From the practical point of view, the reliability of the Enskog theory for mixtures is perhaps more important than for single-component systems, in view of the industrial, biological, and technological applications. The initial application of the Enskog theory to mixtures by Thorne [13] was not entirely satisfactory in that the Onsager reciprocity relations were violated. However, a general reformulation by van Beijeren and Ernst [14] yielded a theory in which the reciprocity relations hold in all cases examined, including mixtures [15]. The resultant theory has been evaluated by Kincaid, Cohen, and Lopez de Haro [16–19] for binary mixtures.

While hard-sphere mixtures have been the subject of a number of Monte Carlo and molecular-dynamics studies relating to their equation of state, few such studies of their transport properties have been made. Except for studies by Alder, Alley, and Dymond [20], Herman and Alder [21], and Subramanian, Levitt, and Davis [22] of the diffusion of a single hard sphere in a hard-sphere fluid having different particle mass and diameter and two studies of self-diffusion at a number of diameter ratios, by Jackson, Rowlinson, and van Swol [23] for the case of equal masses and by Easteal and Woolf [24] for several mass ratios, molecular-dynamics calculations of the transport properties of hard-sphere mixtures have been limited to a single "iostopic" mixture, namely an equimolar mixture having equal diameters and a mass ratio of 0.1 at a volume of three times the close-packed volume. The mutual diffusion coefficient for this case was evaluated by Kincaid and Erpenbeck [25] using both nonequilibrium and Green-Kubo methods, yielding values in good agreement with each other but some 15% greater than the Enskog value. In a more extensive calculation for the same system using the Green-Kubo method [26], referred to hereafter as I, we found the shear viscosity to agree rather well with the Enskog theory, but the thermal conductivity, thermal-diffusion coefficient, and the mutual-diffusion coefficient were significantly larger than the theory by 22%, 27%, and 12%, respectively.

In the present paper we extend these calculations to an equimolar mixture which resembles helium-xenon mixtures in having a mass ratio of 0.03 and a diameter ratio of 0.4. Within the limitation of relatively low density, we treat, then, a case in which effects from the dissimilarity of the species should be more important.

In Sec. II we describe the system briefly, while in Sec. III we review the methods for obtaining the transport coefficients, relying on I for a full description of both the Green-Kubo and Enskog-theory methods. In Sec. IV we describe our results, particularly with respect to finite-system and long-time-tail effects. We close in Sec. V with a discussion.

II. SYSTEM

The system consists of N particles at temperature T, contained in a cubic volume $V=L^3$, subject to periodic boundary conditions. The particles are of n_s types, with N_1 having mass m_1, N_2 having mass $m_2, \ldots,$ and N_{n_s} having mass m_{n_s}, subject to

$$N=\sum_{a=1}^{n_s} N_a ,$$

where we introduce subscripts, $a, b, \ldots$ for the species indices which run from 1 to n_s. The particles interact through a pairwise-additive, central potential, $u_{ab}(r)$, between particles of species a and b, separated by a distance r, so that the total potential energy of the system for periodic boundary conditions is

$$U(\mathbf{r}^N)=\tfrac{1}{2}\sum_{\boldsymbol{\nu}}\sum_{i=1}^{N}\sum_{j=1}^{N}{}' u_{s_i s_j}(|\mathbf{r}_{ij}+\boldsymbol{\nu}L|) , \tag{1}$$

in which $\mathbf{r}^N=\{\mathbf{r}_i, i=1,\ldots,N\}$ denotes a point in configuration space, $\mathbf{r}_i$ is the position of particle i, $\mathbf{r}_{ij}=\mathbf{r}_i-\mathbf{r}_j$, the $\boldsymbol{\nu}$ sum ranges over all 3-vectors of signed integers, the s_i denote the species of particle i, and the prime on the i,j sum indicates the exclusion of the $i=j$ terms for $\boldsymbol{\nu}=0$. In the present study, we limit our attention to the case of hard spheres with "additive" diameters; if σ_a denotes the diameter of particles of species a, then

$$\begin{aligned} u_{ab}(r)&=\phi^{(\mathrm{HS})}(r/\sigma_{ab}) ,\\ \phi^{(\mathrm{HS})}(x)&=\begin{cases}0 & \text{if } x\geq 1\\ \infty & \text{if } x<1 ,\end{cases}\\ \sigma_{ab}&=\frac{\sigma_a+\sigma_b}{2} . \end{aligned} \tag{2}$$

The state of the system is specified by the temperature, density, and the composition. Inasmuch as the thermodynamic and transport properties have their usual trivial dependence on temperature for hard spheres, we need specify only the composition, through n_s-1 mole fractions $x_1, x_2, \ldots, x_{n_s-1}$, and the density, through the reduced volume,

$$\begin{aligned} \tau&=\frac{V}{V_0} ,\\ V_0&=\frac{\sqrt{2}}{2}N\sum_{a=1}^{n_s} x_a\sigma_a^3 . \end{aligned} \tag{3}$$

We note that V_0 reduces to the close-packed volume in the case of a single-component system.

In the present paper we consider only binary mixtures, with the two species characterized by $m_2=0.03m_1$ and $\sigma_2=0.4\sigma_1$. Our calculations are restricted to the equimolar mixture ($x_1=x_2=\frac{1}{2}$) at rather low densities, viz., $\tau=5$, 10, and 20; calculations for higher densities are currently in progress.

III. METHODS

A. Green-Kubo formulation

Our Monte Carlo, molecular-dynamics (MCMD) calculations of the transport coefficients have been described in considerable detail in I; we recapitulate that discussion very briefly here, with several minor notational changes. Transport coefficient L_α is evaluated from the Green-Kubo formula, as the sum of kinetic, cross, and potential terms,

$$L_\alpha=L_\alpha^{(KK)}+L_\alpha^{(K\phi)}+L_\alpha^{(\phi K)}+L_\alpha^{(\phi\phi)} , \tag{4}$$

in which

$$\begin{aligned} L_\alpha^{(AB)}&=\lim_{t\to\infty}\operatorname{tlim}L_\alpha^{(AB)}(t;N) ,\\ L_\alpha^{(AB)}(t;N)&=\int_0^t ds\,\rho_\alpha^{(AB)}(s;N) , \end{aligned} \tag{5}$$

with $A,B\in\{K,\phi\}$, for transport effect $\alpha=\alpha_1\alpha_2\in\{ab,ua,uu,\eta\eta\}$ representing the mutual-diffusion coefficient, the thermal-diffusion coefficient, the thermal conductivity, and the shear viscosity, respectively. Here tlim denotes the thermodynamic limit of large system size and the $\rho_\alpha^{(AB)}(t;N)$ are time-correlation functions of the form,

$$\rho_\alpha^{(AB)}(t;N)=\frac{\beta}{V}\langle\mathcal{J}_{\alpha_1}^{(A)}(0)\mathcal{J}_{\alpha_2}^{(B)}(t)\rangle , \tag{6}$$

in which $\beta=1/(k_BT)$, k_B is the Boltzmann constant, and $\mathcal{J}_{\alpha_i}^{(K)}$ and $\mathcal{J}_{\alpha_i}^{(\phi)}$ are the kinetic and potential parts of the total microscopic currents,

$$\mathcal{J}_{\alpha_i} = \mathcal{J}^{(K)}_{\alpha_i} + \mathcal{J}^{(\phi)}_{\alpha_i} .$$

The angular brackets denote an average over an equilibrium, statistical mechanical ensemble.

As was emphasized in I, the thermal-transport process can be described in a number of different ways, depending on the choice of macroscopic driving forces for the transport of heat and composition. For each such choice, one obtains different expressions for the macroscopic currents, all consistent with the Onsager reciprocity relations. Each choice leads to different, but related, transport coefficients. At the microscopic level, these choices are reflected in different expressions for the microscopic currents $\mathcal{J}_{\alpha_i}$ appearing in the Green-Kubo expressions. In I, the three sets of choices detailed originally by de Groot [27] were explored. It was found that the so-called "mainstream" choice of forces, viz. $-(\nabla T)/T$ and $-T\nabla(\mu_a/T)$, in which μ_a is the specific chemical potential of species a, is advantageous for molecular-dynamics calculations in the sense that neither the thermal wavelength of the atoms nor the partial specific enthalpies are needed to obtain the transport coefficients. Moreover, if the thermal wavelengths and the partial enthalpies are known, then one can readily obtain the so-called "prime" and "double-prime" coefficients from the mainstream coefficients. In the present paper, then, we also compute these mainstream coefficients.

While it is common to emphasize the role of the time-correlation functions $\rho^{(AB)}_\alpha(t;N)$ in discussing the Green-Kubo method, the integrated "time-dependent transport coefficients" $L^{(AB)}_\alpha(t;N)$, Eq. (5), are directly related to the transport coefficients and can be directly calculated by interchanging the order of the time integration in Eq. (5) and the ensemble average in Eq. (6) to obtain

$$L^{(AB)}_\alpha(t;N) = \frac{\beta}{V}\langle \mathcal{J}^{(A)}_{\alpha_1}(0)\mathcal{G}^{(B)}_{\alpha_2}(t)\rangle , \tag{7}$$

in which

$$\mathcal{G}^{(A)}_{\alpha_i}(t) = \int_0^t ds\, \mathcal{J}^{(A)}_{\alpha_i}(s) . \tag{8}$$

Moreover, the related correlation function,

$$M^{(AB)}_\alpha(t;N) = \frac{\beta}{V}\langle \mathcal{J}^{(A)}_{\alpha_1}(t)\mathcal{G}^{(B)}_{\alpha_2}(t)\rangle , \tag{9}$$

can be shown using the Liouville theorem, the time-reversal invariance of trajectories, and the detailed form of the various microscopic currents, to satisfy

$$M^{(AB)}_\alpha(t;N) = L^{(AB)}_\alpha(t;N) \tag{10}$$

in both the canonical and the microcanonical ensembles.

Finally, we note the importance of the Einstein-type functions,

$$S^{(AB)}_\alpha(t;N) = \frac{1}{2t}\frac{\beta}{V}\langle \mathcal{G}^{(A)}_{\alpha_1}(t)\mathcal{G}^{(B)}_{\alpha_2}(t)\rangle , \tag{11}$$

in the evaluation of transport coefficients, for one easily sees from Eq. (10) that

$$\frac{d}{dt}[tS^{(AB)}_\alpha(t;N)] = \tfrac{1}{2}[L^{(AB)}_\alpha(t;N) + L^{(BA)}_\alpha(t;N)] . \tag{12}$$

The Einstein-type functions are widely used in the calculation of self-diffusion because the microscopic current $\mathcal{J}_D$ is the velocity of a single particle, which can be integrated explicitly to yield $\mathcal{G}_D(t) = \Delta\mathbf{R}_i(t)$, the displacement of the particle in the infinite-checkerboard representation, whence $S_D(t)$ is the mean-square displacement divided by $2t$, in this case. For other transport processes, the integral, Eq. (8), cannot generally be evaluated in closed form, so that one expects to evaluate the $\mathcal{G}_{\alpha_i}(t)$ in a molecular-dynamics calculation by numerical integration.

For the case of hard spheres, however, the Einstein-type correlation functions take on particular importance in that the potential parts of the heat current $\mathcal{J}_u$ and the momentum current $\mathcal{J}_\eta$ reduce to sums of terms containing δ functions in the time, $\delta(t - t_\gamma)$, where t_γ is the time of the γth collision, so that only the $\mathcal{G}^{(\phi)}_{\alpha_i}(t)$ are useful for numerical averaging in this case. As a result, $L^{(\phi K)}_{\eta\eta}$, $L^{(\phi\phi)}_{\eta\eta}$, $L^{(\phi K)}_{uu}$, $L^{(\phi\phi)}_{uu}$, and $L^{(\phi K)}_{u1}$ [as well as the corresponding $M^{(AB)}_\alpha(t)$] cannot be computed directly through molecular-dynamics calculations.

B. Numerical determination

In order to estimate the time-correlation functions discussed above, we use a combination of Monte Carlo and molecular-dynamics averaging. For a two-point function of the time such as we have before us, $F(\mathbf{x}^N(t_1), \mathbf{x}^N(t_2))$, in which $\mathbf{x}^N = (\mathbf{r}^N, \mathbf{p}^N)$ denotes a point in phase space and $\mathbf{p}^N$ a point in momentum space, we evaluate the time-correlation function

$$f(t) = \langle F(\mathbf{x}^N(0), \mathbf{x}^N(t))\rangle$$

through the phase and time averages,

$$\bar{f}(t) = \frac{1}{N_{\mathrm{tr}}}\sum_{p=1}^{N_{\mathrm{tr}}}\frac{1}{M}\sum_{m=0}^{M-1} F(\mathbf{x}^N_p(m\Delta t), \mathbf{x}^N_p(t + m\Delta t)) , \tag{13}$$

in which $\{\mathbf{x}^N_p(0), p = 1, 2, \ldots, N_{\mathrm{tr}}\}$ is a set of points in phase space generated by a Monte Carlo procedure, each of which forms the starting point for a dynamical trajectory $\mathbf{x}^N_p(t)$, observed at time $0, h, 2h, \ldots, N_{\mathrm{stp}}h$, with h the observational time step. In the present calculations the Monte Carlo procedure selects a sequence of initial phases from the so-called molecular-dynamics ensemble, the submicrocanonical ensemble having 0 linear momentum in addition to specified N, V, and energy E, the latter defining the temperature through

$$\beta = \frac{3(N-1)}{2E} ,$$

in which $3(N-1)$ is the number of degrees of freedom of the system under the conservation of momentum. The inner sum in Eq. (13) represents a time-average on the pth trajectory, taken over equispaced time origins, $0, \Delta t, 2\Delta t, \ldots,$ with $\Delta t = N_{\mathrm{TO}}h$. The number of such time origins, M, varies with t.

C. Long-time contributions

It is important in evaluating transport coefficients through any molecular-dynamics technique to take account adequately of the effects of the finite size of the systems which are accessible numerically. It has long been recognized that these effects are particularly important in the calculation of transport coefficients in that the time-correlation functions are distorted for values of the time beyond those which characterize the crossing of the finite system by hydrodynamic waves. While there was some expectation that these effects might be less important for the more direct calculation of transport coefficients by nonequilibrium molecular-dynamics methods (so-called NEMD); it now seems clear that finite-size effects are important in both NEMD and Green-Kubo methods [28].

An important element in taking account of finite-N effects for Green-Kubo calculations is the fact that the long-time decay of the time-correlation functions can be determined theoretically through mode-coupling theory. While the simple mode-coupling contributions may not always dominate at the longest times accessible in MD calculations (as in the case of the shear viscosity at high density [5,29]), it does provide a useful framework for making these corrections, as shown, for example, by the recent combination of Green-Kubo molecular dynamics and the mode-coupling theory in determining the self-diffusion coefficient of hard spheres over the entire fluid regime [4]. For the transport coefficients of mixtures, Wood [30] has recently applied the mode-coupling method to determine the long-time tails for the various time-correlation functions which we study here, extending and correcting an earlier calculation by Pomeau [31].

In order to take into account the interrelated effects of finite-system size and the finite time for which the time-correlation functions can be evaluated, we decompose the transport coefficients into short- and long-time contributions,

$$\begin{aligned} L_\alpha &= L_\alpha^{[1]}(t_c) + L_\alpha^{[2]}(t_c)\ , \\ L_\alpha^{[i]}(t_c) &= \mathrm{tlim} L_\alpha^{[i]}(t_c;N)\ , \end{aligned} \tag{14}$$

where t_c is a "crossover" time between the short-time contribution,

$$L_\alpha^{[1]}(t_c;N) = L_\alpha(t_c;N)\ , \tag{15}$$

and the long-time contribution,

$$L_\alpha^{[2]}(t_c;N) = \int_{t_c}^{\infty} dt' \rho_\alpha(t';N)\ , \tag{16}$$

which we assume to approach the theoretical, mode-coupling result in the thermodynamic limit,

$$\begin{aligned} L_\alpha^{[2]}(t_c) &= \int_{t_c}^{\infty} dt\, \rho_\alpha^{(\mathrm{MC})}(t)\ , \\ \rho_\alpha^{(\mathrm{MC})}(t) &= \frac{k_\alpha}{t^{3/2}}\ . \end{aligned} \tag{17}$$

The coefficients k_α are given by Wood [30] and rewritten in I, but not repeated here. They depend on both the equation of state and the transport coefficients of the system. For the former we use the Mansoori-Carnahan-Starling-Leland [32,33] (MCSL) approximation. The transport coefficients are, of course, the objectives of our investigation and it is not entirely clear from the mode-coupling theory which values should be used in the k_α [34]. Here we follow the usual practice (at least at low density) of using the Enskog-theory predictions of Lopez de Haro, Cohen, and Kincaid [16,17,19] as further detailed in I. The evaluation of the transport coefficients in this way also depends on the same approximate equation of state. [We note that here we report only the complete transport coefficients, the sum of the appropriate kinetic, cross, and potential terms, whence we have not continued to notate these distinct components in Eqs. (14)–(17).]

Our justification for using the mode-coupling tail for the large-system, long-time correction to our data depends on the comparison of our observed time-correlation functions, $\rho_\alpha(t;N)$, with the second of Eq. (17). Such a comparison was shown previously for the isotopic mixture of I. We do not show here the comparisons for the present systems but simply observe that they are qualitatively similar to those of I, displaying a general consistency between the theory and MCMD calculations for times greater than roughly 15 mean free times, but with some (not unexpected) apparently significant deviations for times greater than the acoustic-wave-traversal time,

$$t_a = L/c\ , \tag{18}$$

c being the isentropic sound speed. Moreover, we note that even in the case of self-diffusion of hard-spheres for which the calculations are far more accurate and where rather extensive comparisons have been made, the agreement is not definitive [2,3], as emphasized recently in a determination of the hard-sphere self-diffusion coefficient [4].

D. Short-time contributions

The major component of the transport coefficients is the short-time contribution $L_\alpha^{[1]}(t_c)$. As we noted above, the potential contributions, $L_{uu}^{(\phi\phi)}$, $L_{\eta\eta}^{(\phi\phi)}$, $M_{uu}^{(\phi\phi)}$, and $M_{\eta\eta}^{(\phi\phi)}$, cannot be calculated directly because of the singularity of the interaction potential. Thus, our route in the evaluation of the thermal conductivity and the shear-viscosity coefficient is through Eq. (12) and numerical differentiation of the Einstein functions. Our numerical differentiation uses centered first differences, which has the effect of yielding the time-dependent transport coefficients at values of the time intermediate to those for which the directly calculated time-correlation functions are computed. To obtain the cross and kinetic parts of the viscosity and thermal conductivity at the same values of the time, we have computed these from the Einstein functions as well. For the mutual-diffusion coefficient, there are only kinetic contributions and we use the average of the two available estimates,

$$L_{11}^{[1]}(t_c;N) = \tfrac{1}{2}[L_{11}(t_c;N) + M_{11}(t_c;N)]\ .$$

Finally for the thermal-diffusion coefficient, we have averaged four estimates for the kinetic part and two for the cross part

$$L_{u1}^{[1]}(t_c;N)=\tfrac{1}{4}[L_{1u}^{(KK)}(t_c;N)+L_{u1}^{(KK)}(t_c;N)+M_{1u}^{(KK)}(t_c;N)+M_{u1}^{(KK)}(t_c;N)]+\tfrac{1}{2}[L_{1u}^{(K\phi)}(t_c;N)+M_{1u}^{(K\phi)}(t_c;N)]\ .$$

There remain the choice of the crossover time t_c and the extrapolation of the $L_\alpha^{[1]}$ to the thermodynamic limit.

The results are evaluated relative to the Enskog-theory predictions L_α^E, according to the following definitions:

$$\begin{aligned}\hat{\rho}_\alpha(s)&=\frac{t_0\rho_\alpha(st_0)}{L_\alpha^E}\ ,\\ \hat{L}_\alpha^{(AB)}(s)&=\frac{L_\alpha^{(AB)}(st_0)}{L_\alpha^E}\ ,\\ \hat{M}_\alpha^{(AB)}(s)&=\frac{M_\alpha^{(AB)}(st_0)}{L_\alpha^E}\ ,\\ \hat{S}_\alpha^{(AB)}(s)&=\frac{S_\alpha^{(AB)}(st_0)}{L_\alpha^E}\ ,\end{aligned}\tag{19}$$

in which t_0 is the mean free time, a quantity having the known Boltzmann, low-density limit,

$$\begin{aligned}t_{00}&=\frac{N(N-1)}{\sum_a\sum_b N_a(N_b-\delta_{ab})\hat{\sigma}_{ab}^2[(\hat{m}_a+\hat{m}_b)/2\hat{m}_a\hat{m}_b]^{1/2}}t_{00}^{(1)}\ ,\\ t_{00}^{(1)}&=\frac{V}{N(2\sigma_1)^2}\sqrt{m_1\beta/\pi}\ ,\end{aligned}\tag{20}$$

in which $t_{00}^{(1)}$ is the Boltzmann mean free time for pure component 1 at the number density N/V of the mixture, and

$$\hat{m}_a=\frac{m_a}{m_1}\ ,$$

$$\hat{\sigma}_a=\frac{\sigma_a}{\sigma_1}\ .$$

(We note the Boltzmann mean free time was given incorrectly in Eq. (70) of I.) The mean free time can also be evaluated in the MCSL approximation, based on the pair-correlation function at contact [33], which we denote t_0^E. The evaluation of the Enskog transport coefficients in the so-called ninth Enskog approximation was discussed in I.

IV. RESULTS

The Monte Carlo, molecular-dynamics calculations outlined above were made for equimolar binary hard-sphere mixtures having a mass ratio of 0.03 and a diameter ratio of 0.4 for volumes of $5V_0$, $10V_0$, $20V_0$ for several different values of N, from 108 to 4000. Several parameters for these calculations, including the number N_{MC} of attempted Monte Carlo moves per particle between initial configurations for the molecular-dynamics calculation, the number N_{tr} of trajectories, the trajectory length, the time-origin spacing, and the total number N_c of collisions, are given in Table I. The values of N_{MC} are sufficiently large that successive trajectories can be expected to be virtually independent and statistical tests for correlations of functions of the phase support that conclusion. The table also gives the values of the acoustic-wave-traversal time, Eq. (18), for each system, computed from the MCSL equation of state.

Our observations for these systems include the mean free time and the various time-correlation functions discussed above. The latter were evaluated at a sequence of times, $k_1h, 2k_1h, \ldots, n_1k_1h, (n_1k_1+k_2)h, (n_1k_1+2k_2)h, \ldots$, with $h=0.05t_{00}$ and $k_1=1$, $k_2=5$, $k_3=15$, $n_1=30$, $n_2=14$, $n_3=60$, except for the $V=5V_0$, $N=500$ realization for which $n_3=40$. The latter realization was also different from the others in that the thermal diffusion time-correlation functions were not calculated. The maximum times for which the time-correlation functions were evaluated was, then, typically $50t_{00}$ but $35t_{00}$ for $V=5V_0$, $N=500$. We note that for $V=10V_0$ only a

TABLE I. Parameters for the Monte Carlo, molecular-dynamics calculations in the molecular-dynamics ensemble for the transport properties of equimolar mixtures of hard spheres having a diameter ratio of 0.4 and a mass ratio of 0.03. V is the volume and V_0 a reference volume, Eq. (3), N is the number of particles, N_{MC} is the number of Monte Carlo attempted moves per particle between initial states for the trajectories, N_{tr} is the number of distinct trajectories, N_c is the total number of collisions, in millions, N_{stp} is the number of time steps, in thousands, for each trajectory, each step of length $0.05t_{00}$, with t_{00} the Boltzmann mean free time, N_{TO} is the number of steps between time origins, over which the time-correlation functions are averaged. The time-correlation functions are calculated to times as long as t_f, and the once-differenced time-correlation functions extend to times $t_f'=t_f-0.375t_{00}$. The values of the acoustic-wave-traversal time t_a relative to the mean free time t_0 are from the Mansoori-Carnahan-Starling-Leland equation of state [32,33].

V/V_0	N	N_{MC}	N_{tr}	N_c	N_{stp}	N_{TO}	t_f/t_{00}	t_a/t_0
5	108	300	66	29.8	120	5	50	14.7
	500	200	53	36.9	40	5	35	24.6
	1372	300	27	154.4	120	5	50	34.4
10	1372	300	50	240.7	120	5	50	24.1
20	500	300	29	47.0	120	5	50	11.5
	1372	300	30	133.3	120	5	50	16.1
	4000	300	30	97.2	30	5	50	23.0

TABLE II. Results for the Monte Carlo, molecular-dynamics calculations of the mean free time $t_0(N)$ (relative to the Boltzmann value t_{00}) and the time-dependent transport coefficients (relative to the Enskog-theory values), $\hat{L}_\alpha(s_f;N)$, at the longest reduced times s_f or s_f' calculated in the molecular-dynamics ensemble for equimolar mixtures of hard spheres having a diameter ratio of 0.4 and a mass ratio of 0.03, as a function of volume V, relative to a reference volume V_0, and the number of particles N. The infinite-system values are linear least-squares extrapolations in $1/N$. The infinite-system extrapolations for $V=5V_0$, however, are taken at the final time of the $N=500$ calculations, except for $\alpha=u1$ which is taken at $t=50t_{00}$. The numbers in parentheses are the standard deviations in the low-order digit.

V/V_0	N	$t_0(N)/t_{00}$	$\hat{L}_{\eta\eta}(s_f';N)$	$\hat{L}_{uu}(s_f';N)$	$\hat{L}_{u1}(s_f;N)$	$\hat{L}_{11}(s_f;N)$
5	108	0.71783(27)	0.979(11)	0.909(12)	0.924(13)	0.934(11)
	500	0.71893(16)	1.012(20)	0.948(17)		0.917(16)
	1372	0.71995(6)	0.998(22)	0.962(13)	0.951(19)	0.927(17)
	∞	0.72007(7)	1.010(14)	0.967(11)	0.953(21)	0.929(13)
10	1372	0.85512(7)	0.986(15)	0.987(16)	0.993(17)	0.984(14)
20	500	0.92566(18)	1.004(20)	1.005(21)	1.015(23)	1.007(19)
	1372	0.92640(9)	0.964(19)	0.970(20)	0.975(21)	0.978(15)
	4000	0.92622(12)	1.025(36)	1.031(42)	1.034(45)	1.013(36)
	∞	0.92650(11)	0.973(26)	0.978(28)	0.979(30)	0.976(22)

single run, albeit a long one, was made, namely, for a 1372-particle system.

A. Mean free time

The observed values of the mean free time $t_0(N)$ are given in Table II for each system, with statistical uncertainties obtained from the variance among the N_{tr} trajectories. The linear (in $1/N$) least-squares extrapolation of $t_0(N)/t_{00}$ to the thermodynamic limit is also given in Table II for volumes of $5V_0$ and $20V_0$. It is of some interest as a test of our calculations to examine the consistency of the mean free times with the exact low-density limit, viz., the Boltzmann result t_{00}, Eq. (20), as well as the MCSL approximation t_0^E, which reduces to t_{00} at vanishing density. In Fig. 1 we plot the mean free time, reduced by the Boltzmann expression and, in the inset, by the MCSL approximation, for the infinite-system results of Table II for $V=5V_0$ and $20V_0$, along with the 1372-particle value for $V=10V_0$, against the density V_0/V. We note that the infinite-system $V=10V_0$ value is expected to lie at roughly $10^{-4}t_{00}$ above the plotted value on the basis of differences between the 1372 particle and the $N=\infty$ values at $5V_0$ and $20V_0$ given in Table II. Thus, significant deviations from linearity of t_0/t_{00} with density can be detected, leading us to the quadratic fit,

$$\frac{t_0}{t_{00}} = 1 + a_t \frac{V_0}{V} + b_t \left[\frac{V_0}{V} \right]^2 , \tag{21}$$

with coefficients given in Table III and shown by the solid curve in Fig. 1. Evidently the observed values of

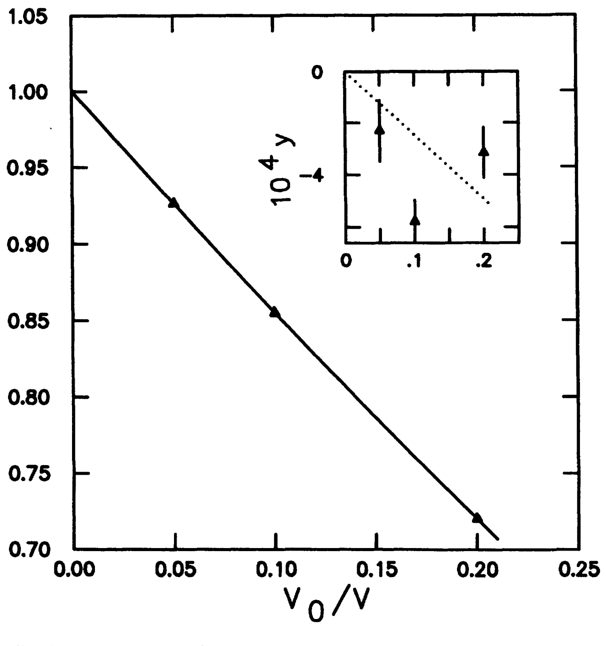

FIG. 1. The mean free time t_0 relative to the Boltzmann value t_{00} as a function of density V_0/V for an equimolar mixture of hard spheres having diameter ratio 0.4 and mass ratio 0.03. Statistical uncertainties are smaller than the plotting symbols. The solid curve is a weighted least-squares fit to Eq. (21). The inset shows the deviation, $y=t_0/t_0^E-1$, from the Mansoori-Carnahan-Starling-Leland value t_0^E, the line is a weighted least-squares fit through the origin, and the error bars are at ± one standard deviation.

TABLE III. The linear coefficients a_α and the quadratic coefficients b_α for the density dependence, Eqs. (21) and (24), of the mean free time (relative to the Boltzmann value) ($\alpha=t$) and the transport coefficients (relative to the Enskog values), viz., shear viscosity ($\alpha=\eta\eta$), thermal conductivity ($\alpha=uu$), thermal diffusion ($\alpha=u1$), and mutual diffusion ($\alpha=11$), for equimolar hard-sphere mixtures having diameter ratios of 0.4 and mass ratios of 0.03, at three values of the volume V relative to the reference volume V_0. The numbers in parentheses are the standard deviations in the low-order digit.

α	a_α	b_α
t	$-1.497(1)$	0.487(7)
$\eta\eta$	0.073(46)	?
uu	$-0.194(44)$	?
$u1$	$-0.185(57)$	?
11	$-0.263(45)$	?

TABLE IV. Enskog-theory predictions L_α^E for the transport coefficients in the ninth Enskog approximation, reduced as in Eq. (22), for equimolar hard-sphere mixtures having diameter ratios of 0.4 and mass ratios of 0.03 at three values of the volume V relative to the reference volume V_0.

V/V_0	$\tilde{L}_{\eta\eta}^E$	$\tilde{L}_{uu}^E$	$\tilde{L}_{u1}^E$	$\tilde{L}_{11}^E$
5	0.283 077 9	9.165 902	−0.081 293 48	0.001 213 527
10	0.214 468 8	10.173 899	−0.095 977 17	0.001 431 648
20	0.198 633 2	10.774 361	−0.103 626 09	0.001 545 728

the mean free time are consistent with the Boltzmann limit but additional results for $V > 10V_0$ would help to demonstrate better the approach.

From the inset in Fig. 1, we note that the deviations of t_0 from MCSL theory appear to be significant, even at these low densities. Indeed, the deviations from the MCSL result appear to be at least marginally significant in the linear term in the density. Again, additional data for $V > 10V_0$ would be helpful in this regard.

B. Transport coefficients

The observed time-dependent transport coefficients at the longest times calculated for each of the systems of Table I are also given in Table II, reduced by the Enskog transport coefficients, as in Eq. (19). The latter were evaluated in the ninth Enskog approximation, as discussed in I; if we define a further reduction of the transport coefficients, $\tilde{L}_\alpha$ through the relations

$$\begin{aligned}
\tilde{L}_{\eta\eta} &= \frac{(m_1\beta)^{1/2}\sigma_1^2}{m_1} L_{\eta\eta} \ , \\
\tilde{L}_{uu} &= \frac{(m_1\beta)^{3/2}\sigma_1^2}{m_1} L_{uu} \ , \\
\tilde{L}_{u1} &= \frac{(m_1\beta)^{1/2}\sigma_1^2}{m_1} L_{u1} \ , \\
\tilde{L}_{11} &= \frac{\sigma_1^2}{m_1(m_1\beta)^{1/2}} L_{11} \ ,
\end{aligned} \qquad (22)$$

then we list the values of the Enskog coefficients $\tilde{L}_\alpha^E$ in Table IV.

As we have seen in Sec. III, the long-time, large-system correction to the transport coefficients are based on the mode-coupling theory, Eq. (17), which yields upon reduction as in Eq. (19), the long-time contribution,

$$\begin{aligned}
\hat{L}_\alpha^{[2]}(s_c) &= \frac{2\hat{k}_\alpha}{s_c^{1/2}} \ , \\
\hat{k}_\alpha &= \frac{k_\alpha}{t_0^{1/2} L_\alpha^E} \ , \\
s_c &= \frac{t_c}{t_0} \ ,
\end{aligned} \qquad (23)$$

with values of the reduced coefficients $\hat{k}_\alpha$ given in Table V.

Perhaps the most straightforward treatment of our data would be to set the crossover time t_c to t_f (or t_f'), extrapolating the $\hat{L}_\alpha(s_f;N)$ to the thermodynamic limit to obtain $\hat{L}_\alpha^{[1]}(s_c)$. For the volume $20V_0$ this has been done to obtain the infinite-system results for that volume given in Table II; the extrapolation was based on a weighted least-squares fit of the $\hat{L}_\alpha(s_f;N)$ linear in $1/N$, shown in Fig. 2. We note that at least at the current level of precision and for our present system sizes, the N dependence of the $\hat{L}_\alpha(s_f;N)$ is not statistically significant.

For the volume $5V_0$, the t_f for the 500-particle system is smaller than that for 108 and 1372 particles. As a result, we chose t_c equal to t_f for $N=500$, viz., $35t_{00}$, and perform the same extrapolation to obtain the infinite-system results for $5V_0$ given in Table II and shown in Fig. 3. Since the $N=500$ calculation did not include the thermal-diffusion coefficient, for this coefficient we chose $t_c = 50t_{00}$; the extrapolation is also shown in Fig. 3. Again we find that the N dependence is at most marginally significant.

For the $10V_0$ case, we have results for the single value $N=1372$. Nonetheless, because the $1/N$ corrections to $\hat{L}_\alpha(s_f;N)$ are found to statistically insignificant for $N=1372$ for the $5V_0$ and $20V_0$ cases, we ignore the $1/N$ extrapolation in this case, using $\hat{L}_\alpha(s_f;1372)$ as $\hat{L}_\alpha(s_f)$. When we combine the $\hat{L}_\alpha^{[1]}$ for each volume with the mode-coupling correction, Eq. (23), we obtain the estimates of the transport in Table VI labeled "$t_c = t_f$."

If we consider the acoustic-wave-traversal times t_a, given in Table I, relative to the t_f also given in Table I,

TABLE V. The reduced mode-coupling coefficients, Eq. (23), for equimolar hard-sphere mixtures having diameter ratios of 0.4 and mass ratios of 0.03 at three values of the volume V relative to the reference volume V_0.

V/V_0	$\hat{k}_{\eta\eta}$	$\hat{k}_{uu}$	$\hat{k}_{u1}$	$\hat{k}_{11}$
5	3.5157×10^{-2}	8.0470×10^{-3}	6.3509×10^{-3}	5.0779×10^{-3}
10	1.6068×10^{-2}	1.3783×10^{-3}	1.1328×10^{-3}	1.0472×10^{-3}
20	4.6704×10^{-3}	2.8748×10^{-4}	2.4794×10^{-4}	2.4598×10^{-4}

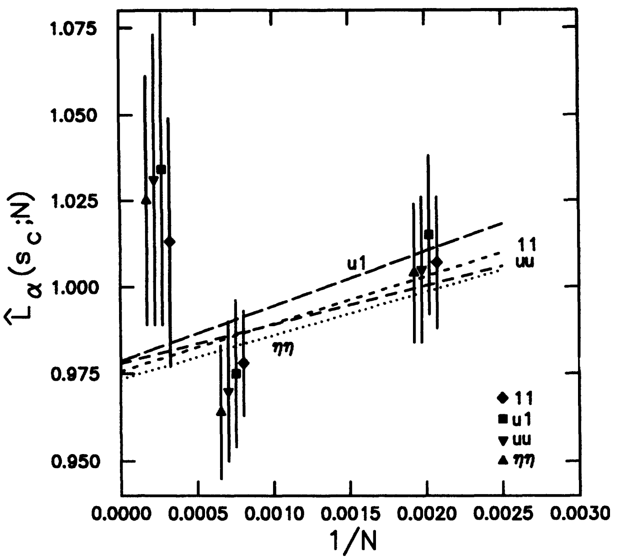

FIG. 2. The time-dependent transport coefficients relative to the Enskog values, $\hat{L}_\alpha(s_c;N)$, for equimolar mixtures of hard spheres having a mass ratio of 0.03 and a diameter ratio of 0.4, at a volume of $20V_0$ as a function of $1/N$, where N is the number of particles, for a crossover time $s_c=t_f/t_0=50t_{00}/t_0$ (with t_0 the mean free time) for the mutual diffusion ($\alpha=11$) and the thermal diffusion ($u1$) and $t_f'/t_0=49.625t_{00}/t_0$ for the shear viscosity ($\eta\eta$) and the thermal conductivity (uu). To display the various error bars, which extend ± one standard deviation, the points are displaced slightly from the $1/N$ abscissa value.

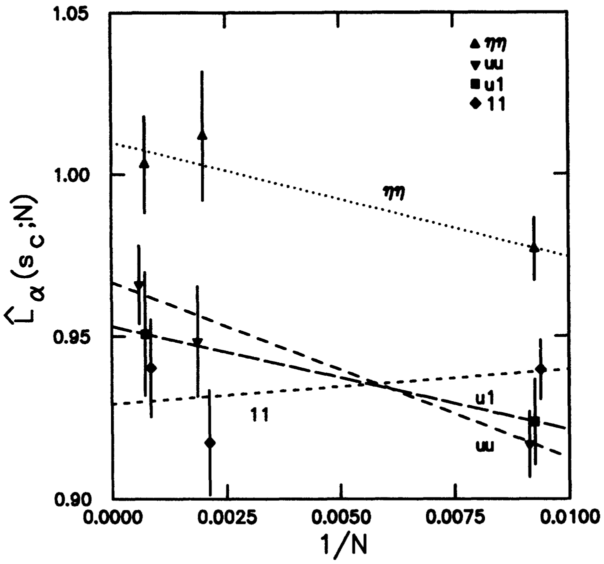

FIG. 3. The time-dependent transport coefficients relative to the Enskog values, $\hat{L}_\alpha(s_c;N)$ as in Fig. 2, at a volume of $5V_0$ for a crossover time $s_c=35t_{00}/t_0$ for thermal diffusion, and $34.625t_{00}/t_0$ for shear viscosity and thermal conductivity.

we might question this procedure for correcting the data in that the time interval (t_a,t_f) is quite appreciable, even for the largest systems for which we have data. Moreover, it seems unlikely the finite-system effects in this interval would actually decay simple as $1/N$ but rather have oscillatory components, as shown for example in the case of the self-diffusion coefficient of hard spheres [4]. This suggests assigning a value to the crossover t_c, that is somewhat smaller than t_a, at least for the largest of the systems studied for a particular reduced volume τ, but large enough that there appears to be agreement between the mode-coupling theory and the data for the largest N. On this basis we choose intermediate crossover times, $t_c=t_{\text{int}}$, viz., $t_c=23t_{00}$ for $5V_0$, $20.75t_{00}$ for $10V_0$, and $15.5t_{00}$ for $20V_0$. The values of $\hat{L}_\alpha(s_{\text{int}};N)$ and their least-squares extrapolations to the thermodynamic limit are shown in Table VII. The latter are then combined with mode-coupling corrections, Eq. (17), to yield the column labeled "$t_c=t_{\text{int}}$" of Table VI. We see that the two sets of values are in statistical agreement in all cases, but we prefer the $t_c=t_{\text{int}}$ set because of the larger values of the $\hat{L}_\alpha$ for $20V_0$. These differences arise not from the slightly larger $\hat{L}_\alpha^{[2]}$ contributions but from the statistically insignificant, but overall negative, contributions from the $\hat{\rho}_\alpha(s;N)$ in the (t_{int},t_f) interval; because the long-time tails are, in fact, positive for the present values of the volume, these negative contributions are almost certainly inappropriate in the large-N limit.

It is of interest to consider the nature of the deviations from the Enskog theory at low density. We therefore fit the $t_c=t_{\text{int}}$ results of Table VI to the form

$$\hat{L}_\alpha=1+a_\alpha\left[\frac{V_0}{V}\right] \tag{24}$$

to obtain the coefficients shown in Table III; the linear fits are shown graphically in Fig. 4. We note that for the transport coefficients we cannot obtain the quadratic correction to Eq. (24), as we did for the mean free time,

TABLE VI. Transport coefficients in the thermodynamic limit relative to the Enskog values $\hat{L}_\alpha$ for equimolar mixtures of hard spheres having a diameter ratio of 0.4 and a mass ratio of 0.03, based on two different choices for the crossover time t_c, as explained in the text. V is the volume and V_0 a reference volume.

V/V_0	5		10		20	
	$t_c=t_f$	$t_c=t_{\text{int}}$	$t_c=t_f$	$t_c=t_{\text{int}}$	$t_c=t_f$	$t_c=t_{\text{int}}$
$\hat{L}_{\eta\eta}$	1.020(14)	1.022(11)	0.990(15)	1.000(9)	0.974(26)	0.998(11)
$\hat{L}_{uu}$	0.967(11)	0.962(10)	0.987(16)	0.983(9)	0.978(28)	0.975(13)
$\hat{L}_{u1}$	0.953(21)	0.956(14)	0.994(17)	0.987(10)	0.979(30)	0.989(15)
$\hat{L}_{11}$	0.929(13)	0.941(11)	0.984(14)	0.980(9)	0.976(22)	0.990(12)

TABLE VII. Time-dependent transport coefficients from the Monte Carlo, molecular-dynamics calculations as in Table II, but for intermediate reduced times, $s_{\mathrm{int}}=t_{\mathrm{int}}/t_0$ and t'_{int}/t_0. For $V=5V_0$, $t_{\mathrm{int}}=23t_{00}$, $t'_{\mathrm{int}}=22.625t_{00}$. For $v=10V_0$, $t_{\mathrm{int}}=20.75t_{00}$, $t'_{\mathrm{int}}=20.375t_{00}$. For $V=20V_0$, $t_{\mathrm{int}}=15.5t_{00}$, $t'_{\mathrm{int}}=15.125t_{00}$.

V/V_0	N	$\hat{L}_{\eta\eta}(s'_{\mathrm{int}})$	$\hat{L}_{uu}(s'_{\mathrm{int}})$	$\hat{L}_{u1}(s_{\mathrm{int}})$	$\hat{L}_{11}(s_{\mathrm{int}})$
5	108	0.978(8)	0.926(9)	0.941(10)	0.945(8)
	500	1.007(17)	0.957(15)		0.927(15)
	1372	1.005(12)	0.955(11)	0.955(13)	0.949(12)
	∞	1.009(11)	0.959(10)	0.956(14)	0.941(11)
10	1372	0.994(9)	0.982(9)	0.986(10)	0.979(9)
20	500	0.987(7)	0.987(10)	0.991(12)	0.986(11)
	1372	0.986(8)	0.980(10)	0.995(10)	0.997(8)
	4000	1.015(17)	0.972(21)	0.970(25)	0.960(19)
	∞	0.996(11)	0.974(13)	0.989(15)	0.990(12)

principally because of the two-orders-of-magnitude increase in the uncertainty in the transport coefficients over that for the mean free time. In addition, the coefficients in Table III measure deviations from the Boltzmann expression for the t_0 but from the Enskog theory for the L_α. This circumstance is indicated in Table III by placing "?" in the b_α column for the transport coefficients. In assessing these deviations from the Enskog theory, we note that the statistical uncertainties given in Table III (for the transport coefficients) are similar in magnitude to the linear coefficients, a_α, and reflect only two degrees of freedom in the least-squares fit. Therefore the 95% confidence interval includes $a_\alpha=0$ when the large uncertainty in the true variance of these distributions is taken into account. Substantial improvement in these estimates will require calculations at additional values of the volume.

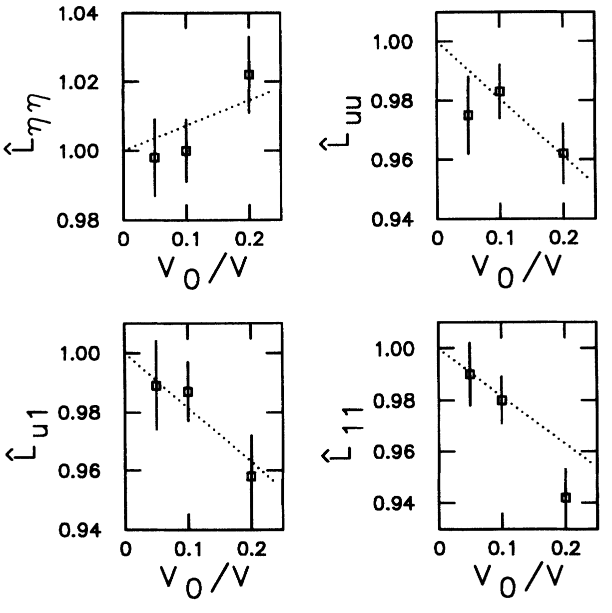

FIG. 4. The transport coefficients relative to the Enskog values L_α as a function of density V_0/V for an equimolar mixture of hard spheres having diameter ratio 0.4 and mass ratio 0.03. The error bars extend ± one standard deviation. In each case, the line is a weighted least-squares fit to Eq. (24).

V. DISCUSSION

The most striking feature of the present results is perhaps the smallness of the deviations from the Enskog theory. While the collisional transfer and two-particle correlation effects which the theory addresses are themselves small at low density, they do become appreciable at moderate density for the single-component hard-sphere fluid. One might easily suppose these effects to be of similar magnitude here so that the present agreement indicates the correctness of the Enskog treatment of these effects.

Secondly, we find (rather weak) evidence that the low-density deviations from the Enskog theory are *negative,* at least for the thermal conductivity, the thermal-diffusion coefficient, and the mutual-diffusion coefficient. If these corrections are indeed negative, they would not appear to be of a hydrodynamic origin as are the long-time tails, for the tail contributions are positive in each case, as seen from the sign of the coefficients in Table V. Moreover, additional caution in interpreting the sign of these density dependences must be recognized in that the deviations are small and at the same time the present evaluation of the Enskog theory is based on the MCSL equation of state, the accuracy of which has not been very thoroughly tested; our observed deviations could simply reflect the inaccuracy of the Enskog calculation, a question which we hope to address in the future.

The importance of additional study of the equation of state of the hard-sphere mixture is also emphasized by our results for the mean free time. The latter appear to deviate rather rapidly from the MCSL theory with increasing density, suggesting the need for additional refinement of the theory.

Finally, we observe that the 2% level of accuracy attained in the present calculations reflects the extensive Monte Carlo and time averaging used. (Roughly 500 h of Cray-1 and Cray-YMP CPU time were required.) This level of accuracy is to be contrasted with 0.2% achieved in the calculation of the self-diffusion coefficient of single-component hard spheres at low density, based on calculations which were an order of magnitude shorter (as measured by the total number of collisions). At higher densities we can expect to require more extensive averaging to continue the 2% accuracy, particularly if long-time-tail effects become important.

ACKNOWLEDGMENTS

The author is grateful to J. M. Kincaid of the State University of New York at Stony Brook for making his computer program for computing the Enskog transport coefficients available to me and for the continued encouragement of W. W. Wood of Los Alamos. This work was supported by a contract with the U. S. Department of Energy, Office of Basic Sciences, Division of Chemical Sciences.

[1] B. J. Alder, D. M. Gass, and T. E. Wainwright, J. Chem. Phys. **53**, 3813 (1970).

[2] J. J. Erpenbeck and W. W. Wood, Phys. Rev. A **26**, 1648 (1982).

[3] J. J. Erpenbeck and W. W. Wood, Phys. Rev. A **32**, 412 (1985).

[4] J. J. Erpenbeck and W. W. Wood, Phys. Rev. A **43**, 4254 (1991).

[5] J. J. Erpenbeck and W. W. Wood, J. Stat. Phys. **24**, 455 (1981).

[6] J. R. Dorfman and E. G. D. Cohen, Phys. Rev. A **6**, 776 (1972).

[7] J.R. Dorfman and E. G. D. Cohen, Phys. Rev. A **12**, 292 (1975).

[8] M. H. Ernst, E. H. Hauge, and J. M. J. van Leeuwen, Phys. Rev. A **4**, 2055 (1971).

[9] M. H. Ernst, E. H. Hauge, and J. M. J. van Leeuwen, J. Stat. Phys. **15**, 7 (1976).

[10] T. R. Kirkpatrick, Phys. Rev. Lett. **53**, 1735 (1984).

[11] H. van Beijeren, Phys. Lett. **105A** , 191 (1984).

[12] I. M. de Schepper, A. F. Haffmans, and H. van Beijeren, Phys. Rev. Lett. **57**, 1715 (1986).

[13] S. Chapman and T. G. Cowling, *The Mathematical Theory of Nonuniform Gases,* 2nd ed. (Cambridge University Press, Cambridge, 1952).

[14] H. van Beijeren and M. H. Ernst, Physica **68**, 437 (1973).

[15] H. van Beijeren and M. H. Ernst, Physica **70**, 225 (1973).

[16] M. Lopez de Haro, E. G. D. Cohen, and J. M. Kincaid, J. Chem. Phys. **78**, 2746 (1983).

[17] J. M. Kincaid, M. Lopez de Haro, and E. G. D. Cohen, J. Chem. Phys. **79**, 4509 (1983).

[18] M. Lopez de Haro and E. G. D. Cohen, J. Chem. Phys. **80**, 408 (1984).

[19] J. M. Kincaid, E. G. D. Cohen, and M. Lopez de Haro, J. Chem. Phys. **86**, 937 (1987).

[20] B. J. Alder, W. E. Alley, and J. H. Dymond, J. Chem. Phys. **61**, 1415 (1974).

[21] P. T. Herman and B. J. Alder, J. Chem. Phys. **56**, 987 (1972).

[22] G. Subramanian, D. Levitt, and H. Davis, J. Chem. Phys. **60**, 591 (1974).

[23] G. Jackson, J. S. Rowlinson, and F. van Swol, J. Phys. Chem. **91**, 4907 (1987).

[24] A. J. Easteal and L. A. Woolf, Chem. Phys. **88**, 101 (1984).

[25] J. M. Kincaid and J. J. Erpenbeck, J. Chem. Phys. **84**, 3418 (1986).

[26] J. J. Erpenbeck, Phys. Rev. A **39**, 4718 (1989).

[27] S. R. de Groot, *Thermodynamics of Irreversible Processes* (North-Holland, Amsterdam, 1951).

[28] D. J. Evans, G. P. Morriss, and L. M. Hood, Mol. Phys. **68**, 637 (1989).

[29] D. J. Evans, J. Stat. Phys. **22**, 81 (1980).

[30] W. W. Wood, J. Stat. Phys. **57**, 675 (1989).

[31] Y. Pomeau, J. Chem. Phys. **57**, 2800 (1972).

[32] G. A. Mansoori, N. F. Carnahan, K. E. Starling, and T. W. Leland, J. Chem. Phys. **54**, 1523 (1971).

[33] T. M. Reed and K. E. Gubbins, *Applied Statistical Mechanics* (McGraw-Hill, New York, 1973).

[34] I. M. de Schepper and M. H. Ernst, Physica **87A**, 35 (1977).